

# Open loop V/f Control of Induction Motor based on hybrid PWM With reduced torque ripple

M. Harsha Vardhan Reddy

Department of Electrical and Electronics Engineering,  
Karunya University,  
Coimbatore- 641114, India  
e-mail: maramreddyharsha@gmail.com

V.Jegathesan

Department of Electrical and Electronics Engineering,  
Karunya University,  
Coimbatore- 641114, India  
e-mail: jegathesan@karunya.edu.

**Abstract**—Voltage source inverter (VSI) fed induction motors are widely used in variable speed applications. Space Vector Pulse Width Modulation (SVPWM) has become the successful techniques to construct three phase sine wave Voltage Source Inverter (VSI) parallel to control three-phase induction motor using v/f control. Because of the low maintenance and robustness induction motors have many applications in the industries. The speed control of induction motor is more important to achieve maximum torque and efficiency. VSI fed induction motor produces a pulsating torque due to the application of non sinusoidal voltages. Among the various modulation strategies Space Vector pulse width Modulation Technique is the efficient one because it has better spectral performance and output voltage is more closed to sinusoidal. Torque pulsation is strongly influenced by PWM technique used. This paper compares the torque ripples of convectional space vector PWM with hybrid PWM techniques. In hybrid PWM both continuous PWM and discontinuous PWM techniques are employed. The open loop V/f control of induction motor with hybrid PWM shows better reduction in torque ripples when compared with conventional space vector PWM technique. The simulated design is tested using MATLAB 7.8.

**Keywords**—Hybrid PWM, SVPWM, Inverter, Induction Motor, Torque Ripples.

## I. INTRODUCTION

SPACE vector pulse width modulation technique has been widely investigated for decades. Space Vector Modulation (SVM) Technique was originally developed as a vector approach to Pulse Width Modulation (PWM) for three-phase inverters. It is a more sophisticated technique for generating sine wave that provides a higher voltage to the motor with lower total harmonic distortion [1-3]. It gives a higher output Voltage for the same dc-bus voltage, lower switching losses, and better harmonic performance. For the ac machine drive application, full utilization of the dc bus voltage is extremely important in order to achieve the maximum output torque under all operating conditions in this aspect, compared with any other PWM method for the voltage source inverter, the PWM method based on voltage space vectors results in excellent dc bus utilization. Moreover as compared to sine triangle PWM method, the current ripple in steady state operation can minimized in this method. It confines space vectors to be applied according to the region where the output voltage vector is located. The main aim of pulse width modulation technique is to obtain

variable output having a maximum fundamental component with minimum harmonics. The space vector modulation technique is more popular than conventional technique because of the following features

- Higher efficiency
- It has lower base band harmonics than regular PWM or other sine based modulation methods, or otherwise optimizes harmonics.
- SVM increases the output capability of SPWM without distorting line-line output voltage waveform
- 15% more output voltage can be obtained than conventional modulation techniques.

Therefore SVPWM scheme becomes the preferred PWM technique for various three-phase power converter applications. With SVPWM [4-7] the performance of IM is improved because it eliminates all the lower order harmonics in the output voltage of the inverter (stator voltage of the IM) when compared to the conventional SPWM technique.

A three-phase voltage source inverter produces eight switching states, comprising two zero states and six active states, as shown in Fig. 1(a). The corresponding voltage vectors are normalized with respect to DC bus voltage. As shown in Fig.1,  $V_{ref}$  is represented by using two active vectors  $V_1$  and  $V_2$  and zero vectors  $V_0$  and  $V_7$ . So the sequence used to represent  $V_{ref}$  in sector I is 0127.  $T_1$  and  $T_2$  are times for which vectors  $V_1$  and  $V_2$  are applied,  $T_z$  is the time for which zero vectors  $V_0$  and  $V_7$  are applied.  $T_z$  is divided into two equal halves between  $V_0$  and  $V_7$ . i.e  $T_z/2$ . This method of representation of  $V_{ref}$  is considered as continuous modulating technique [8-10].

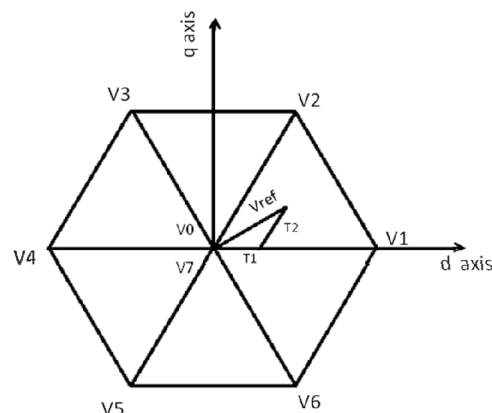


Fig.1 voltage vectors of voltage source inverter

The active and zero vector times are described as follows in equation (1)

$$\begin{aligned} T_1 &= \frac{v_{ref} \sin(\pi/3 - \alpha)}{\sin(\pi/3)} T_s \\ T_2 &= \frac{v_{ref} \sin(\alpha)}{\sin(\pi/3)} T_s \\ T_z &= T_s - T_1 - T_2 \end{aligned} \quad (1)$$

Discontinuous PWM techniques uses only one zero state in the sub cycle and the active state is applied twice in the sub cycle. Only 2-phases are conducting at a time i.e  $120^\circ$  clamping in the each phase in the sub cycle. Therefore in hybrid PWM [11-12] techniques the both continuous and discontinuous PWM techniques are combined. In this paper the torque ripples of induction motor is reduced by hybrid PWM technique. The different space vector based sequences used to generate the switching pulse for hybrid PWM are 0127, 1012, 2721, 012, 721.

## II. IMPLEMENTATION OF SVPWM

For all the above mentioned sequence calculating Vref, angle( $\alpha$ ), sector and times T1, T2 and Tz is same. The switching time for different switches changes with different sequences. The switching time of switches S1, S3, S5 with sequence 0127 in sector I are given in Fig.2

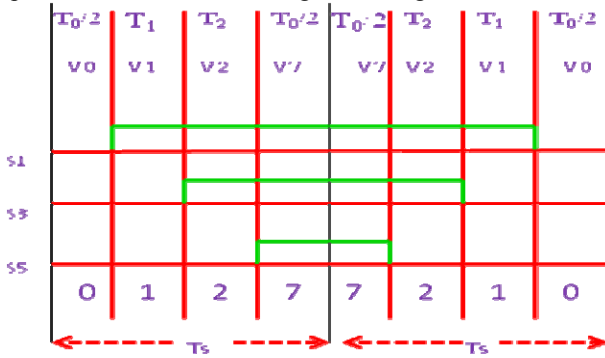


Fig.2 switching times of sequence 0127

Similarly it can be generalized for remaining sectors. In the Fig.2, there are 3-switchings in the sub cycle and the 0 and 7 states are also divided in to two equal halves. The switching time for the sequence 0127 is given by equation (2).

$$T_s = 1/(2f_s) \quad (2)$$

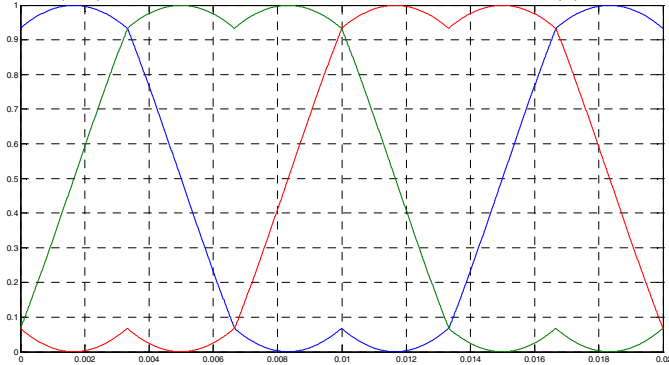


Fig.3 Modulating wave for the sequence 0127

The modulating wave for the sequence 0127 is shown in fig.3. The modulating wave is similar to the third harmonic injected wave. Because of this property the SVPWM is best when compared with SPWM.

The implementation of SVPWM technique with other sequence carried out by taking one zero vector instead of two zero vectors as in convectional SVPWM. The sequence possible is 012. The switching time of switches S1, S3, S5 with sequence 012 are given in Fig.4

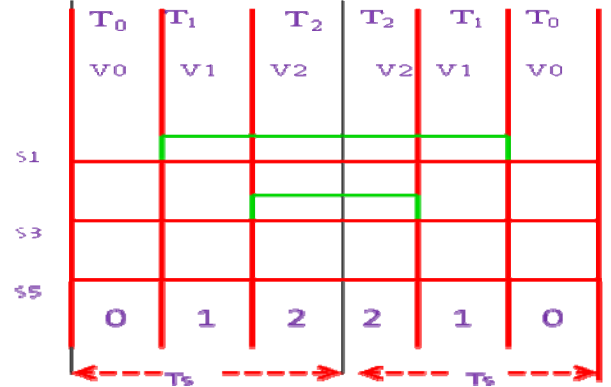


Fig.4 Switching times of sequence 012

With sequence 012 only 2-switchings are possible in the sub cycle. The sub cycle duration of 012 sequence is less than the 0127 sequence. This reduction of the sub cycle duration could lead to reduced RMS torque ripple and RMS current ripple at high values of Vref. The switching time for the sequence 012 is given in equation (3)

$$T_s = 1/(3f_s) \quad (3)$$

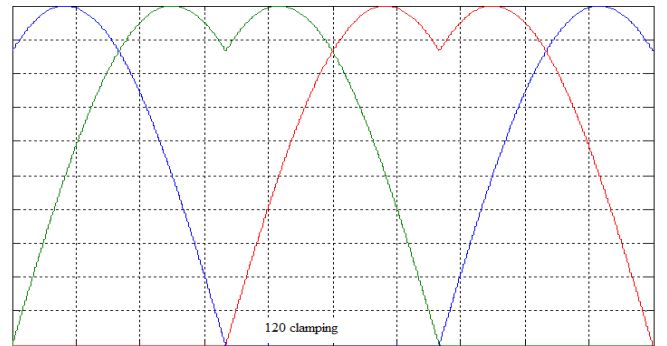


Fig.5 modulating wave for the sequence 012 and 1012

The modulating wave for the sequence is shown in Fig.5. The modulating waveform for the sequence 012 sequence is discontinuous as shown in Fig.5. Each phase is clamped for  $120^\circ$ . So in this sequence only two phases are conducting at any instant.

The implementation of SVPWM technique with other sequence is carried out by dividing active vector in to two equal halves instead of dividing zero vectors in to two equal halves as in convectional SVPWM. The sequence possible is 1012. The switching time of switches S1, S3, S5 with sequence 1012 are given in Fig.6.

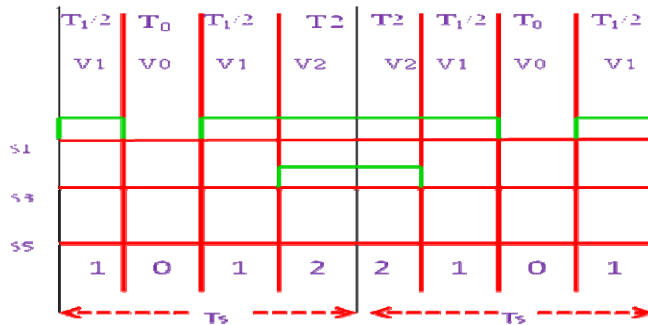


Fig.6 Switching times of sequence 1012

The modulating waveform for the 1012 sequence is also discontinuous as shown in Fig.5. Each phase is clamped for  $120^\circ$ . So in this sequence only two phases conduct at each instant of time. In sequence 1012 1-phase double switches within the sub cycle. This kind of double switching operation is not possible in sequences like 0127 and 012.

For the sequence 012 and 0127 the modulating waveform are compared with triangular waveform for pulse generation.

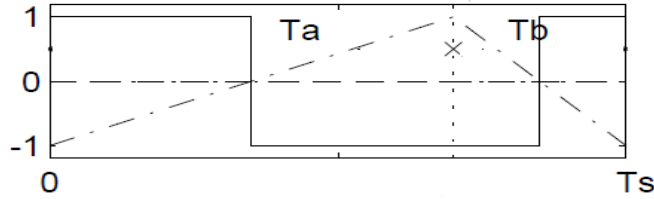


Fig.7 triangular comparison for the sequence 1012

In the sequence 1012, the modulating waveform is compared with two ramps signals, which constitute this signal, having different slopes. They divide the sub cycle into two unequal durations, namely Ta and Tb, as shown in Fig.7 Their relative slopes change with change in the average pole voltage. The modulating wave varies with both Vref and  $\alpha$ . Thus, the signal required for comparison is dependent on both Vref and  $\alpha$ . This kind of comparison is only for double switching phase.

### III. CALCULATION OF STATOR FLUX RIPPLE

The applied voltage vector equals the reference voltage vector only in an average sense over the given sub cycle, and not in an instantaneous fashion. The difference between the reference vector and the instantaneous applied voltage vector is the instantaneous error voltage vector. The error voltage vector calculation is shown in Fig.8 and given in equation

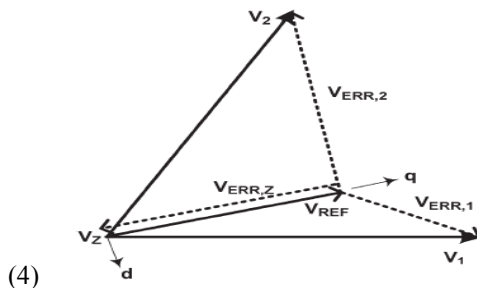


Fig.8 Error voltage vectors in sector I

$$V_{rip,1} = V_1 - V_{REF}$$

$$V_{rip,2} = V_2 - V_{REF}$$

$$V_{rip,Z} = -V_{REF}$$

(4)

When these error voltages are resolved in to q-axis and d-axis the corresponding d and q axis equations are given in equation (5).

$$Q_1 = (2/3 V_{dc} \cos \alpha - V_{ref}) * T_1$$

$$Q_2 = (2/3 V_{dc} \cos(\alpha - 60) - V_{ref}) * T_2$$

$$Q_z = -V_{ref} * T_z$$

$$D_1 = 2/3 * V_{dc} \sin \alpha * T_1$$

(5)

Sum of all d and q-axis error voltages is zero, indicating balance between applied volt-seconds and reference volt-seconds over a sub cycle.

The time integral of the error voltage vector, referred to as ‘stator flux ripple vector’, is a measure of the ripple in the line current of the converter. In practice rms value of the stator flux ripple over a sub cycle is a measure of the rms current ripple over the given sub cycle.

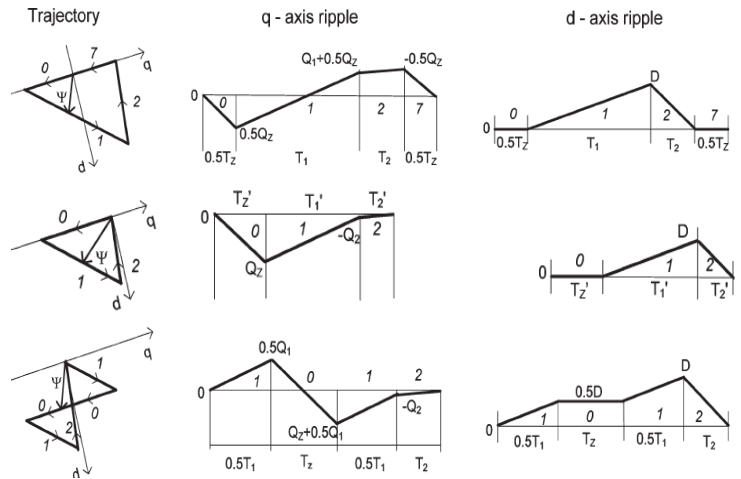


Fig.9 stator flux ripple vector over the sub cycle for the sequence 0127, 012 and 1012

Fig.9 shows the stator flux ripple vector over the sub cycle for three sequences for a given reference voltage. The q-axis and d-axis ripple are shown separately in Fig.9. Since the voltage reference vector is aligned with the q-axis and the stator resistance drop is negligible, there is a steady flux only along the d-axis. This steady flux interacts with the ripple current along the q-axis to produce the ripple torque. Hence, the torque ripple is practically independent of the d-axis current ripple (since there is no steady flux along the q-axis), while being proportional to the q-axis current ripple.

The mean square value of the q-axis current ripple over the given sub cycle for the sequence 0127, 1012, 2721, 012 and 721 are given equation 6(a-e) .

$$I_{q\_0127}^2 = 1/12 * Qz^2 * T_z / T_s + 1/3 * [0.25 * Qz^2 + 0.5 * Qz * (0.5 * Qz + Q1) + (0.5 * Qz + Q1)^2] * T_1 / T_s + 1/3 * [0.25 * Qz^2 - 0.5 * Qz * (0.5 * Qz + Q1) + (0.5 * Qz + Q1)^2] * T_2 / T_s \quad (6a)$$

$$I_{q\_1012}^2 = 1/6 * [0.25 * Q1^2 + (0.5 * Q1 + Qz)^2 + (0.5 * Q1 + Qz) * (Q1 + Qz) + (Q1 + Qz)^2] * T_1 / T_s + 1/3 * [(0.5 * Q1 + Qz)^2 + (0.5 * Q1 + Qz) * 0.5 * Q1 + 0.25 * Q1^2] * T_z / T_s + 1/3 * (Q1 + Qz)^2 * T_2 / T_s \quad (6b)$$

$$I_{q\_2721}^2 = 1/6 * [0.25 * Q2^2 + (0.5 * Q2 + Qz)^2 + (0.5 * Q2 + Qz) * (Q2 + Qz) + (Q2 + Qz)^2] * T_2 / T_s + 1/3 * [(0.5 * Q2 + Qz)^2 + (0.5 * Q2 + Qz) * 0.5 * Q2 + 0.25 * Q2^2] * T_z / T_s + 1/3 * (Q2 + Qz)^2 * T_1 / T_s \quad (6c)$$

$$I_{q\_012}^2 = [(Qz^2 * T_z) + Qz^2 + ((Qz * (Qz + Q1)) + (Qz + Q1)^2 * T1) + (Qz + Q1)^2 * T2] * (1/3 * T_s) \quad (6d)$$

$$I_{q\_721}^2 = [(Qz^2 * T_z) + ((Qz^2 + (Qz * (Qz + Q2)) + (Qz + Q2)^2 * T1) + (Qz + Q2)^2 * T2] * (1/3 * T_s) \quad (6e)$$

There is one more sequence known as optimal sequence in which the zero vectors is divided in to two un equal halves. This division of zero vectors is based on optimal value of 'x' Where

$$x_{opt} = \frac{(T_z + T_2)}{2T_s} - \frac{Q1}{Qz} \frac{(T_1 + T_2)}{2T_s}$$

Therefore

$$T_0 = xT_z$$

$$T_7 = (1 - x)T_z$$

In general if it is divided in to two equal halves then  $x=0.5$ .

#### IV. HYBRID PWM METHODS

The stator flux ripple values for the different sequences 0127, 1012, and 2721 are shown in Fig.9. From the Fig.9, for lower sector angles, 1012 sequence has less stator flux ripple. For medium sector angle, 0127 sequence has less ripple, and for higher sector angle 2721 shows less stator ripple in the sector I that is  $0^\circ < \alpha < 60^\circ$ .

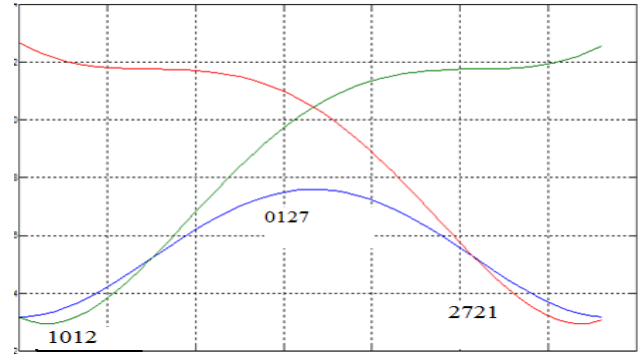


Fig.10 Stator flux ripple comparison of sequence 0127, 1012 and 2721

From the Fig.9 and Fig.10, different sequences have less stator ripple at different angles in the sector. The combination of all these sequences for sector I are given in Fig.11. The sector is divided in to three regions. The region A, 1012 has less ripple, in the region B, 0127 has less ripple, and in the region C 2721 has less ripple. The combined SVPWM sequences called hybrid PWM which has much effect at high modulation index. At low modulation index all the sequence has same effect.

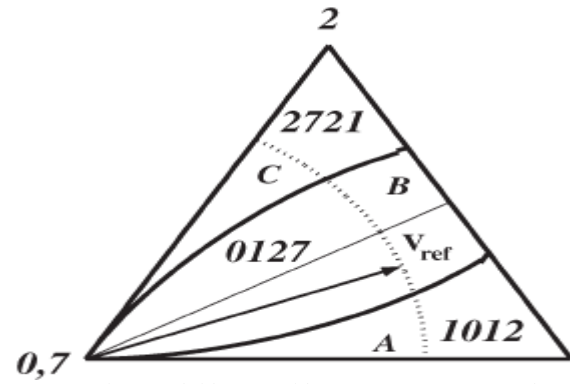


Fig.11 Hybrid PWM with sequence 0127, 1012 and 2721

When sequence 012, 721 and optimal 0127 sequence are compared against their q-axis ripple, the sequence which has low ripple in sector I at different regions are shown in Fig.12

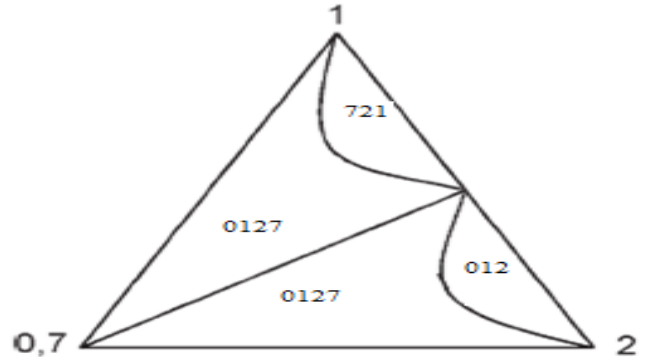


Fig.12 Hybrid PWM with sequence 012, 721, optimal 0127

## V. SIMULATION RESULTS

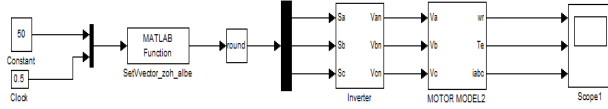


Fig.13 open loop V/f control of induction motor

The SIMULINK model of hybrid PWM is shown in fig.13. In the open loop system the frequency is taken as input to V/f control for all voltage conversion and pulse generation. The sub systems of open loop control are coding for pulse generation, inverter modeling and induction motor modeling.

TABLE 1 MOTOR PARAMETERS

Rated speed	1500 RPM	Rotor resistance	0.94Ω
frequency	50HZ	Voltage (DC)	600V
Stator resistance	0.94Ω	Mutual inductance	176mH
Stator inductance	183mH	Rotor inductance	183mH

The inverter and induction motor are modeled using SIMULINK. The torque plots for conventional SVPWM by sequence 0127 and hybrid PWM using sequence 012, 721, and optimal 0127 sequence at modulation index  $M=0.9$  are shown in Fig.14.

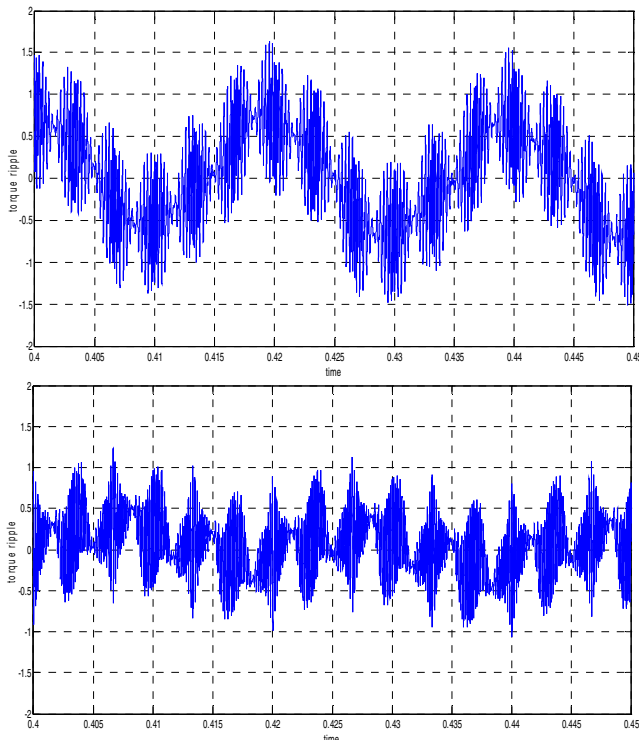


Fig.14 Torque plot for conventional SVPWM (0127) and hybrid PWM with sequence 012, 721, optimal 0127 on no load

The torque plots for conventional SVPWM by sequence 0127 and hybrid PWM using sequence 1012, 2721, optimal 0127 sequence at modulation index  $M=0.9$  are shown in Fig.15.

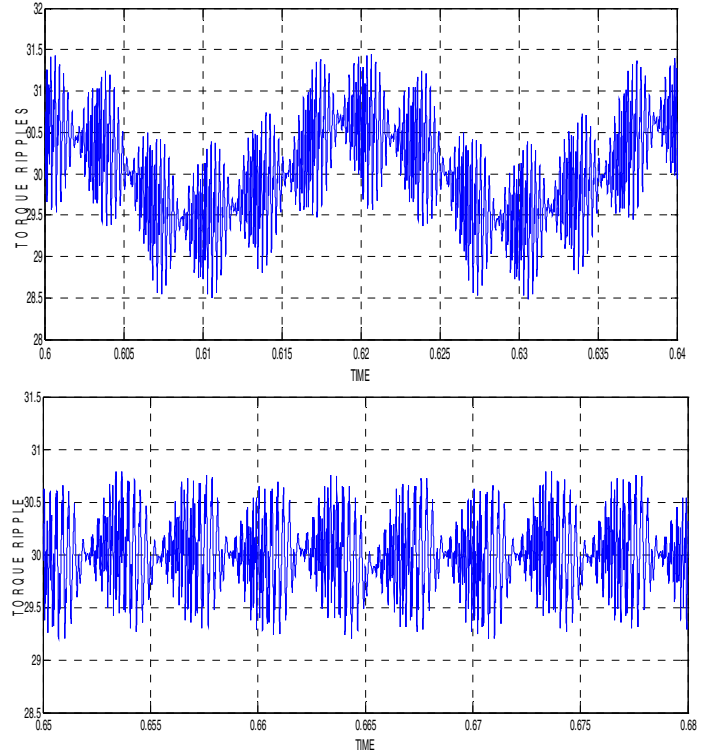


Fig.15 Torque plot with convectional SVPWM (0127) and hybrid PWM with sequence 1012, 2721, 0127 with Torque=30N-m open loop

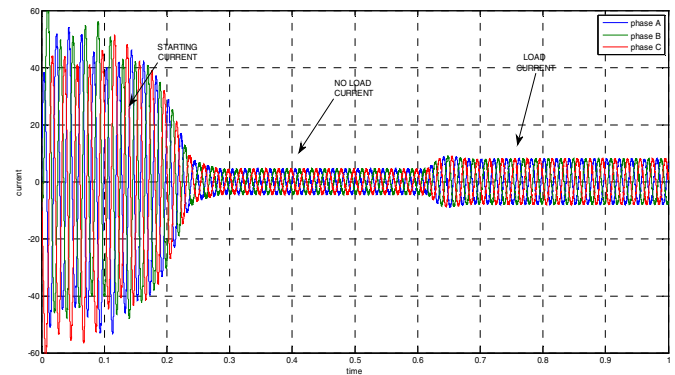


Fig.16 Current plot of hybrid PWM

The current plot for hybrid PWM by sequence 1012, 2721, 0127 are shown in Fig.16 at modulation index  $M=0.9$ .

From the results, the torque ripple is reduced in hybrid PWM technique when compared to the convectional PWM with sequence 0127. By using the sequence 0127, 1012, 2721 only torque ripple is reduced. Only small change in current ripple i.e THD of sequence 0127 is 7.18% but the THD of the hybrid PWM with sequence 0127, 1012, 2721 is 7.11%. The hybrid PWM with sequence 012, 721 and optimal 0127 is 6.15%. The hybrid PWM with sequence

012,721 and optimal 0127 both current ripple and torque ripple are reduced. But the reduction of torque ripples is better with sequence 0127, 1012, 2721 in closed loop v/f control.

## VI. CONCLUSION

The hybrid PWM techniques has been proposed for reduction of torque ripple in voltage source inverter fed induction motor drives. It is shown that hybrid PWM has less torque ripple when compared with convectional PWM methods. In hybrid PWM with 0127, 1012 and 2721 has low torque ripple but hybrid PWM with sequence 012, 721 and optimum 0127 sequence has less torque ripple and current ripple. When we compare only torque ripple 0127, 1012 and 2721 is better than other hybrid PWM. The results show that reduction in torque ripples with improvement in harmonic distortion in current due to the hybrid PWM when compared with convectional SVPWM.

## REFERENCES

- [1] Keliang Zhou and Daniel Wang, Member, IEEE; "Relationship between Space Vector Modulation and three phase Carrier-Based PWM, A Comprehensive Analysis"; *IEEE Transactions on Industrial Electronics*, Vol. 49, No. 1, February 2007.
- [2] Mr. Alexandru Savulescu; "The analysis and the simulation of SVM signal generator used for the control of electric drives with asynchronous drives"; Oct 4-6, *ICEP 2008*.
- [3] Dr. Vaishnavi Deshpande, Mr. J.G. Chaudhary; "Development and Simulation of SVPWM and SPWM induction motor drives"; *ICETET-2009*.
- [4] Guilian Guo, Wenxia You; "Quality Analysis of SVPWM inverter output voltage"; *International Conference of Computer Science and Software Engineering 2008*.
- [5] R. Linga Swamy, P. Satish Kumar; "Speed Control of Space Vector Modulated Inverter Control Induction Motor Drive"; *IMECS 2008*, 19-21 March 2008, Hong Kong.
- [6] T. G. Habetler et al., "Direct torque control of induction machines using space vector modulation," *IEEE Trans. Ind. Applicat.*, vol. 28, pp. 1045–1053, Sept./Oct. 1992.
- [7] Jin-woo jung project on "space vector pwm inverter" date: february 20, 2005.
- [8] K. Basu, J. S. S. Prasad, and G. Narayanan, "Minimization of torque ripple in PWM ac drives," *IEEE Trans. Ind. Electron.*, vol. 56, no. 2, pp. 553–558, Feb. 2009.
- [9] G. Narayanan, D. Zhao, H. K. Krishnamurthy, R. Ayyanar, and V. T. Ranganathan, "Space vector based hybrid PWM techniques for reduced current ripple," *IEEE Trans. Ind. Electron.*, vol. 55, no. 4, pp. 1614–1627, Apr. 2008.
- [10] K. Basu, "Minimization of torque ripple in space vector PWM based induction motor drives," M.Sc. (Engg.) thesis, Indian Inst. Sci., Bangalore, India, 2005.
- [11] G. Narayanan and V. T. Ranganathan, "Analytical evaluation of harmonic distortion in PWM ac drives using the notion of stator flux ripple," *IEEE Trans. Power Electron.*, vol. 20, no. 2, pp. 466–474, Mar. 2005.
- [12] T. Brahmananda Reddy, J. Amarnath and D. Subbarayudu, "Improvement of DTC performance by using hybrid space vector pulsewidth modulation algorithm" *International Review of Electrical Engineering*, Vol.4, no.2, pp. 593-600, Jul-Aug, 2007.